HHS Public Access

Author manuscript

*Nature*. Author manuscript; available in PMC 2012 June 22.

Published in final edited form as:

*Nature*. ; 480(7378): 547–551. doi:10.1038/nature10648.

# Floor plate-derived dopamine neurons from hESCs efficiently engraft in animal models of PD

**Sonja Kriks**[1,2,*], **Jae-Won Shim**[1,2,*], **Jinghua Piao**[1,3], **Yosif M. Ganat**[1,2], **Dustin R. Wakeman**[4], **Zhong Xie**[5], **Luis Carrillo-Reid**[5], **Gordon Auyeung**[1,3], **Chris Antonacci**[1,3], **Amanda Buch**[1,3], **Lichuan Yang**[6], **M. Flint Beal**[6], **D. James Surmeier**[5], **Jeffrey H. Kordower**[4], **Viviane Tabar**[1,3], and **Lorenz Studer**[1,2,3]

[1]Center for Stem Cell Biology, Memorial Sloan-Kettering Cancer Center, 1275 York Ave, New York, NY 10065, USA

[2]Developmental Biology Program, Memorial Sloan-Kettering Cancer Center, 1275 York Ave, New York, NY 10065, USA

[3]Department of Neurosurgery, Memorial Sloan-Kettering Cancer Center, 1275 York Ave, New York, NY 10065, USA

[4]Department of Neurological Sciences, Rush University Medical Center, Chicago, IL 60612, USA

[5]Department of Physiology, Feinberg School of Medicine, Northwestern University, Chicago, Illinois, IL 60611, USA

[6]Department of Neurology and Neuroscience, Weill Medical College of Cornell University, New York Presbyterian Hospital, 525 East 68th Street, F610, New York, NY 10021, USA

## SUMMARY

Human pluripotent stem cells (hPSCs) are a promising source of cells for applications in regenerative medicine. Directed differentiation of hPSCs into specialized cells such as spinal motoneurons[1] or midbrain dopamine (DA) neurons[2] has been achieved. However, the effective use of hPSCs for cell therapy has lagged behind. While mouse PSC-derived DA neurons have shown efficacy in models of Parkinson's disease (PD)[3, 4], DA neurons from human PSCs generally display poor *in vivo* performance[5]. There are also considerable safety concerns for hPSCs related to their potential for teratoma formation or neural overgrowth[6, 7]



Correspondence: Dr. Lorenz Studer, Center for Stem Cell Biology, Developmental Biology Program & Department of Neurosurgery, Memorial Sloan-Kettering Cancer Center, 1275 York Ave, Box 256, New York, NY 10065, Phone 212-639-6126, FAX: 212-717-3642, studerl@mskcc.org.

*equally contributed

**AUTHOR CONTRIBUTIONS**

S.K. and J.-W.S.: conception and study design, maintenance and directed differentiation of hPSCs, cellular/molecular assays, histological analyses, mouse behavioral assays, data interpretation and writing of manuscript; J.P., G.A., C.A., A.B. rat transplantation, histological analyses and behavioral assays. Y.M.G.: mouse transplantation and histological analyses. D.R.W., J.K.: monkey transplantation, histological analysis and data interpretation. L.Y., M.F.B: HPLC analysis and data interpretation. L.C., Z.X and J.S.: electrophysiological analyses and data interpretation. V.T.: study design, data analysis and writing of manuscript; L.S.: conception and study design, data analysis and interpretation, writing of manuscript.

Here we present a novel floor plate-based strategy for the derivation of human DA neurons that efficiently engraft *in vivo*, suggesting that past failures were due to incomplete specification rather than a specific vulnerability of the cells. Midbrain floor plate precursors are derived from hPSCs in 11 days following exposure to small molecule activators of sonic hedgehog (SHH) and canonical WNT signaling. Engraftable midbrain DA neurons are obtained by day 25 and can be maintained *in vitro* for several months. Extensive molecular profiling, biochemical and electrophysiological data define developmental progression and confirm identity of hPSC-derived midbrain DA neurons. *In vivo* survival and function is demonstrated in PD models using three host species. Long-term engraftment in 6-OHDA-lesioned mice and rats demonstrates robust survival of midbrain DA neurons, complete restoration of amphetamine-induced rotation behavior and improvements in tests of forelimb use and akinesia. Finally, scalability is demonstrated by transplantation into Parkinsonian monkeys. Excellent DA neuron survival, function and lack of neural overgrowth in the three animal models indicate promise for the development of cell based therapies in PD.

---

Recent mouse genetic studies have demonstrated an important role for the transcription factor *FOXA2* during midbrain DA neuron development[8, 9]. A unique feature of the developing midbrain is the co-expression of the floor plate (FP) marker FOXA2 and the roof plate marker LMX1A. Normally, FP and roof plate cells are located at distinct positions in the CNS (ventral versus dorsal) and exhibit diametrically opposed patterning requirements[10, 11]. We recently reported the derivation of FP precursors from hESCs[12] using a modified dual-SMAD inhibition protocol[13]. Canonical Wnt signaling is important for both, roof plate function[14] and midbrain DA neuron development[15]. We therefore hypothesized that WNT activation may induce LMX1A expression and neurogenic conversion of hPSC-derived midbrain FP towards DA neuron fate. Here we report that exposure to CHIR99021 (CHIR), a potent GSK3b inhibitor known to strongly activate WNT signaling[16], induces LMX1A in FOXA2+ FP precursors (Figure 1a). CHIR was much more potent than recombinant Wnt3A or Wnt1 at inducing LMX1A expression (data not shown). The efficiency of LMX1A induction was dependent on the timing of CHIR exposure with a maximum effect from day 3–11 (Supplementary Figure 1). CHIR was the most critical factor for inducing co-expression of FOXA2/LMX1A, while other factors such as FGF8 had only marginal effects (Supplementary Figure 2). Induction of FOXA2/LMX1A co-expression required strong activation of SHH signaling using purmorphamine, a small molecule agonist, alone or in combination with recombinant SHH (Supplementary Figure 3). Treatment with SHH agonists (purmorphamine + SHH) and FGF8 (S/F8) in the absence of CHIR99021 showed significantly lower expression of FOXA2 by day 11 and complete lack of LMX1A expression (Figure 1a,b). Dual SMAD inhibition (exposure to LDN193189 + SB431542 = "LSB") did not yield FOXA2-expressing cells, but a subset of LMX1A+ cells (Figure 1a,b). The anterior marker OTX2 was robustly induced in LSB and LSB/S/F8/CHIR treated cultures, but not under LSB/S/F8 conditions (Figure 1a,c). Systematic comparisons of the three culture conditions (Figure 1d) were performed using global temporal gene expression profiling. Hierarchical clustering of differentially expressed genes segregated the three treatment conditions by day 11 of differentiation (Supplementary Figure 4a). *FOXA1, FOXA2* and several other SHH downstream targets including *PTCH1* were amongst the most differentially regulated transcripts in LSB/S/F8/CHIR versus LSB treatment sets

(Figure 1e). Expression of *LMX1A, NGN2,* and *DDC* indicated establishment of midbrain DA neuron precursor fate already by day 11 (Figure 1e,f). In contrast, LSB cultures were enriched for dorsal forebrain precursor markers such as *HES5, PAX6, LHX2, and EMX2.* Direct comparison of LSB/S/F8/CHIR versus LSB/S/F8 treatment (Figure 1f) confirmed selective enrichment for midbrain DA precursor markers in LSB/S/F8/CHIR group and suggested hypothalamic precursor identity in LSB/S/F8 treated cultures based on the differential expression of *RAX1, SIX3*, and *SIX6*[17] (see also *POMC, OTP* expression in Figure 2d below). The full list of differentially expressed transcripts Supplementary Tables 1,2 and gene ontology analysis Supplementary Figure 4b (DAVID; http://david.abcc.ncifcrf.gov[18]) confirmed enrichment for canonical WNT signaling upon CHIR treatment (raw data available at GEO http://www.ncbi.nlm.nih.gov/geo/ accession#: GSE32658). Comparative temporal gene expression analysis for markers of midbrain DA precursors (Figure 1g) versus anterior and ventral non-DA fates (Figure 1h) partitioned the three induction conditions into: i) LSB: dorsal forebrain; ii) LSB/S/F8: ventral / hypothalamic; iii) LSB/S/F8/CHIR: midbrain DA identity.

By day 25, all three conditions yielded Tuj1+ neurons (Figure 2a) and cells expressing TH, the rate-limiting enzyme in the synthesis of DA. However, only the LSB/S/F8/CHIR group yielded TH+ cells co-expressing LMX1A and FOXA2 as well as the nuclear receptor NURR1 (NR4A2) (Figure 2a,b). Comparing gene expression in day 13 versus day 25 cultures confirmed robust induction of postmitotic DA neuron markers (Figure 2c). Characterizing DA neuron identity at day 25 in comparison to LSB and LSB/S/F8 showed enrichment for known midbrain DA neuron transcripts and identified multiple novel candidate markers (Figure 2d, Supplementary Tables 3–5, Supplementary Figure 4b). For example, the transcript most highly enriched in LSB/S/F8/CHIR (midbrain DA group) was *TTF3*, a gene not previously associated with midbrain DA neuron development, but highly expressed in the human substantia nigra (Supplementary Figure 4c; Allen Brain Atlas: http://human.brain-map.org). Similar data were obtained for *EBF-1*, *EBF-3* (Supplementary Figure 4c) as well as *TTR*, a known transcriptional target of FOXA2 in the liver[19]. We observed enrichment of several *PITX* genes, and *PITX3*, a classic marker of midbrain DA neurons, was also expressed robustly at day 25 of differentiation (Figure 2e). Finally, both midbrain FP and DA neuron induction was readily reproduced in independent hESC and hiPSC lines (Supplementary Figure 5). Our data demonstrate that the LSB/S/F8/CHIR protocol yields cells expressing a marker profile matching midbrain DA neuron fate.

We next proceeded to determine the *in vitro* and *in vivo* properties of FP-derived DA neurons in comparison to DA neurons obtained via a neural rosette intermediate[3] (Supplementary Figure 6). Patterning of neural rosettes represents the currently most widely used strategy for deriving DA neurons from hPSCs[2, 6, 20]. Both FP- and rosette-based protocols were efficient at generating TH+ neurons capable of long-term *in vitro* survival (day 50 of differentiation; Figure 3a). However, the percentage of TH+ cells was significantly higher in FP-derived cultures (Figure 3b). While TH+ cells in both protocols displayed co-expression of NURR1, only FP-derived DA neurons co-expressed FOXA2 and LMX1A (Figure 3a,b). Few GABA and serotonin (5-HT)-positive neurons were observed (Figure 3c). DA, and its metabolites DOPAC and HVA, were present in cultures generated

with either protocol, but DA levels were ~ 8 times higher in FP cultures (Figure 3d,e). Midbrain DA neurons exhibited extensive fiber outgrowth and robust expression of mature neuronal markers including synapsin, dopamine transporter (DAT), and G-protein coupled, inwardly rectifying potassium channel (Kir3.2 – also called GIRK2 – expressed in substantia nigra pars compacta (SNpc) DA neurons) (Figure 3f, Supplementary Figure 7).

SNpc DA neurons *in vivo* exhibit an electrophysiological phenotype that differentiates them from most other neurons in the brain. In particular, they spike spontaneously at a slow (1–3 Hz) rate. Moreover, this slow spiking is accompanied by a slow, sub-threshold oscillatory potential [21, 22]. After 2–3 weeks *in vitro*, these same physiological features are displayed by SNpc DA neurons cultured from early postnatal mice (data not shown). The DA neurons differentiated from hESCs consistently (4/4) displayed this distinctive physiological phenotype (Figure 3g-i). Future studies will be required to determine whether all features of SNpc DA neurons are recapitulated by the hESC DA neurons *in vitro* or whether full differentiation will require maturation *in vivo*. However, our data indicate that FP derived DA neurons do exhibit the cardinal physiological features of mature SNpc DA neurons.

A major challenge in the field has been the ability to generate hPSC-derived midbrain DA neurons that functionally engraft *in vivo* without the risk of neural overgrowth[7] or inappropriate differentiation into non-midbrain neurons[23]. Based on fetal tissue transplantation studies[24] we hypothesized that the time of cell cycle exit, marked by expression of NURR1[25], may be a suitable stage for grafting (~day 25 of differentiation - Figure 2). Initial studies using day 25 cells in non-lesioned adult mice showed robust survival of hPSC-derived FOXA2+/TH+ neurons at 6 weeks after transplantation (Supplementary Figure 8). We next addressed whether FOXA2+/TH+ cells survive long-term in Parkinsonian hosts without resulting in neural overgrowth. To this end, we made 6-hydroxy-dopamine (6-OHDA) lesions[3] in *NOD-SCID IL2Rgc* null mice, a strain that efficiently supports xenograft survival with particular sensitivity for exposing rare tumorigenic cells[26]. Both FP- and rosette-derived cultures were grafted ($150\times10^3$/animal) without prior purification in order to reveal potential contaminating cells with proliferative potential. Four and a half months after transplantation FP-derived DA neuron grafts showed a well-defined graft core composed of TH+ cells co-expressing FOXA2 and the human specific marker hNCAM (Figure 4a-c). Functional analysis showed a complete rescue of amphetamine-induced rotation behavior. In contrast, rosette-derived grafts had few TH+ neurons, did not produce significant reductions in rotation behavior (Figure 4d) and displayed massive neural overgrowth (graft volume > 20 $mm^3$; Supplementary Figure 9). Extensive overgrowth reported here as compared to previous work with rosette-derived DA grafts[27,28] is likely due to the longer survival periods (4.5 months versus 6 weeks), lack of FACS purification prior to transplantation and choice of *NOD-SCID IL2Rgc* null host. The number of proliferating Ki-67+ cells was minimal in FP-derived grafts (< 1% of total cells), while rosette-derived grafts retained pockets of proliferating neural precursors. Neural overgrowth is thought to be caused by primitive anterior neuroectodermal cells within the graft[6, 29]. This hypothesis was supported by the expression of the forebrain marker FOXG1 in rosette- but not FP-derived grafts. A small percentage of astroglial cells were present in

both FP- and rosette-derived grafts, though most GFAP+ cells were negative for human markers indicating host origin (Supplementary Figure 9).

Our results in *NOD-SCID IL2Rgc* null mice demonstrated robust long-term survival of FOXA2+/TH+ neurons, complete reversal of amphetamine-induced rotation behavior and lack of neural overgrowth. However, some of these outcomes could be attributable to the specific use of *NOD-SCID IL2Rgc* null mice. To test this hypothesis, FP-derived DA neuron cultures ($250 \times 10^3$ cells) were transplanted in adult 6-OHDA lesioned rats immunosuppressed pharmacologically using cyclosporine A. Five months after transplantation graft survival was robust (Figure 4e-h) with an average of more than 15,000 TH+ cells co-expressing FOXA2 (Figure 4g), and human nuclear antigen (hNA) (Figure 4e); TH+/hNCAM+ fibers emanated from the graft core into the surrounding host striatum (Figure 4f). In addition to FOXA2, TH+ cells expressed midbrain DA neuron markers PITX3 and NURR1 (Figure 4h-j). Behavioral analyses showed complete rescue of amphetamine-induced rotational asymmetry in contrast to sham-grafted animals (Figure 4k). Grafted animals also showed improvements in the stepping test (Figure 4l) measuring forelimb akinesia and in the cylinder test (Figure 4m), assays that do not depend on pharmacological stimulation of the DA system. The late onset of recovery (~ 3–4 months after transplantation) is expected for human DA neurons and depends on the rate of *in vivo* maturation including levels of DAT expression (Figure 4n). The presence of TH+ cells expressing Kir3.2 channels (GIRK2) or calbindin indicate that both SNpc (A9) and ventral tegmental area (A10) DA neurons are present in the graft (Figure 4o,p). As in mice (Supplementary Figure 9), serotonergic and GABAergic cells were rare (< 1% of total cells), as were the mostly host-derived GFAP+ glial cells (7 % of total cells; (Supplementary Figure 10). While few serotonin+ neurons were detected in the graft, we observed hNCAM-negative, likely host-derived serotonergic fibers (Supplementary Figure 10).

Our results demonstrate excellent graft survival and behavioral outcome in two independent murine models. However, the number of DA neurons required in a mouse or rat brain represents only a fraction of the cells needed in a human. To test the scalability of our approach, we performed pilot grafting studies in two adult MPTP lesioned rhesus monkeys. We readily obtained batches of $50 \times 10^6$ transplantable DA neuron precursors by day 25 of differentiation using the FP-based protocol. Cells were injected at three locations (posterior caudate and pre-commissural putamen) on each side of the brain (6 tracts in total, $1.25 \times 10^6$ cells/tract), and the animals were immunosuppressed with cyclosporine-A. One side of the brain was injected with DA precursors from a GFP expressing subclone of H9, while the other side was engrafted with cells derived from unmarked H9 cells. One month after transplantation, we observed robust survival of midbrain DA neurons based on expression of GFP (Supplementary Figure 11) and the human specific cytoplasmic marker (SC-121) (Figure 4q). Each graft core was surrounded by a halo of TH+ fibers extending up to 3 mm into the host (Figure 4r). The graft cores were composed of TH+ neurons co-expressing SC-121 (Figure 4s) and FOXA2 (Figure 4t). Areas within the graft contained Iba1+ host microglia (Supplementary Figure 11) indicating incomplete immunosuppression.

In conclusion, we present a novel FP-based hPSC differentiation protocol that faithfully recapitulates midbrain DA neuron development. Access to cells with the cardinal features of

midbrain DA neurons will enable a broad range of biomedical applications such as basic developmental studies, high-throughput drug discovery and PD-iPSC based disease modeling. Importantly, our study establishes a means of obtaining a scalable source of FOXA2+/TH+ neurons for neural transplantation a major step on the road towards considering a cell based therapy for PD.

## Methods Summary

Human ESC (H9, H1) and iPSC lines (2C6 and SeV6) were subjected to a modified dual SMAD-inhibition[13] based FP induction[12] protocol. Exposure to SHH C25II, Purmorphamine, FGF8 and CHIR99021 were optimized for midbrain FP and DA neuron yield (see Figure 1d). Following FP induction, further maturation was carried out in Neurobasal/B27 medium supplemented with AA, BDNF, GDNF, TGFβ3 and dbcAMP (see full methods for details). The resulting DA neurons were subjected to extensive phenotypic characterization via immunocytochemistry, qRT-PCR, gene expression profiling, HPLC analysis for DA and *in vitro* electrophysiological recordings. *In vivo* studies were performed in 6-hydroxydopamine lesioned, hemiparkinsonian rodents (adult *NOD-SCID IL2Rgc* mice and Sprague Dawley rats) as well as in two adult rhesus monkeys treated with carotid injections of MPTP. DA neurons were injected stereotactically in the striata of the animals ($150 \times 10^3$ cells in mice, $250 \times 10^3$ cells in rats) and a total of $7.5 \times 10^6$ cells (distributed in 6 tracts; 3 on each side of brain) in monkeys. Behavioral assays were performed at monthly intervals post grafting, including amphetamine mediated rotational analysis as well as a test for focal akinesia (“stepping test”) and forelimb use (cylinder test). Rats and mice were sacrificed at 18–20 weeks and the primates at 1 month post grafting. Characterization of the grafts was performed via stereological analyses of cell numbers and graft volumes and comprehensive immunohistochemistry.

## Supplementary Material

Refer to Web version on PubMed Central for supplementary material.

## Acknowledgments

We thank K. Manova (MSKCC molecular cytology core), M. Tomishima (SKI stem cell core), A. Viale (MSKCC genomics core) for excellent technical support, and R. McKay for Nestin antibody. The work was supported by NIH/NINDS grant NS052671, the European Commission project NeuroStemcell, the Starr foundation and NYSTEM contract C024414 to L.S.; by NYSTEM contract C024413, the Michael T. McCarthy Foundation, and the Elkus Family Foundation to V.T.; by the Consolidated Anti-Aging Foundation to J.H.K.; by NIH/NINDS grant P50 NS047085, and support from Falk Medical Research Trust to D.J.S.. J.-W.S. was supported by NYSCF (Druckenmiller fellowship) and S.K. by Starr stem cell scholar fellowship.

## References

1. Li XJ, et al. Specification of motoneurons from human embryonic stem cells. Nat Biotechnol. 2005; 23:215–221. [PubMed: 15685164]
2. Perrier AL, et al. From the Cover: Derivation of midbrain dopamine neurons from human embryonic stem cells. Proc Natl Acad Sci U S A. 2004; 101:12543–8. [PubMed: 15310843]
3. Tabar V, et al. Therapeutic cloning in individual Parkinsonian mice. Nature Med. 2008; 14:379–381. [PubMed: 18376409]

4. Wernig M, et al. Neurons derived from reprogrammed fibroblasts functionally integrate into the fetal brain and improve symptoms of rats with Parkinson's disease. Proc Natl Acad Sci U S A. 2008; 105:5856–5861. [PubMed: 18391196]
5. Lindvall O, Kokaia Z. Stem cells in human neurodegenerative disorders--time for clinical translation? J Clin Invest. 2010; 120:29–40. [PubMed: 20051634]
6. Elkabetz Y, et al. Human ES cell-derived neural rosettes reveal a functionally dinstinct early neural stem cell stage. Genes Dev. 2008; 22:152–165. [PubMed: 18198334]
7. Roy NS, et al. Functional engraftment of human ES cell-derived dopaminergic neurons enriched by coculture with telomerase-immortalized midbrain astrocytes. Nature Med. 2006; 12:1259–1268. [PubMed: 17057709]
8. Kittappa R, Chang WW, Awatramani RB, McKay RD. The foxa2 gene controls the birth spontaneous degeneration of dopamine neurons in old age. PLoS Biol. 2007; 5:e325. [PubMed: 18076286]
9. Ferri AL, et al. Foxa1 and Foxa2 regulate multiple phases of midbrain dopaminergic neuron development in a dosage-dependent manner. Development. 2007; 134:2761–2769. [PubMed: 17596284]
10. Roelink H, et al. Floor plate and motor neuron induction by vhh-1, a vertebrate homolog of hedgehog expressed by the notochord. Cell. 1994; 76:761–775. [PubMed: 8124714]
11. Liem KF, Tremml G, Roelink H, Jessell TM. Dorsal differentiation of neural plate cells induced by BMP-mediated signals from epidermal ectoderm. Cell. 1995; 82:969–979. [PubMed: 7553857]
12. Fasano CA, Chambers SM, Lee G, Tomishima MJ, Studer L. Efficient derivation of functional floor plate tissue from human embryonic stem cells. Cell Stem Cell. 2010; 6:336–347. [PubMed: 20362538]
13. Chambers SM, et al. Highly efficient neural conversion of human ES and iPS cells by dual inhibition of SMAD signaling. Nat Biotechnol. 2009; 27:275–280. [PubMed: 19252484]
14. Muroyama Y, Fujihara M, Ikeya M, Kondoh H, Takada S. Wnt signaling plays an essential role in neuronal specification of the dorsal spinal cord. Genes Dev. 2002; 16:548–553. [PubMed: 11877374]
15. Joksimovic M, et al. Wnt antagonism of Shh facilitates midbrain floor plate neurogenesis. Nat Neurosci. 2009; 12:125–131. [PubMed: 19122665]
16. Lyashenko N, et al. Differential requirement for the dual functions of beta-catenin in embryonic stem cell self-renewal and germ layer formation. Nat Cell Biol. 2011; 13:753–761. [PubMed: 21685890]
17. VanDunk C, Hunter LA, Gray PA. Development, maturation, and necessity of transcription factors in the mouse suprachiasmatic nucleus. J Neurosci. 2011; 31:6457–6467. [PubMed: 21525287]
18. Huang, dW; Sherman, BT.; Lempicki, RA. Systematic and integrative analysis of large gene lists using DAVID bioinformatics resources. Nat Protoc. 2009; 4:44–57. [PubMed: 19131956]
19. Costa RH, Grayson DR, Darnell JE Jr. Multiple hepatocyte-enriched nuclear factors function in the regulation of transthyretin and alpha 1-antitrypsin genes. Mol Cell Biol. 1989; 9:1415–1425. [PubMed: 2786140]
20. Soldner F, et al. Parkinson's disease patient-derived induced pluripotent stem cells free of viral reprogramming factors. Cell. 2009; 136:964–977. [PubMed: 19269371]
21. Guzman JN, Sanchez-Padilla J, Chan CS, Surmeier DJ. Robust pacemaking in substantia nigra dopaminergic neurons. J Neurosci. 2009; 29:11011–11019. [PubMed: 19726659]
22. Nedergaard S, Flatman JA, Engberg I. Nifedipine- and omega-conotoxin-sensitive Ca2+ conductances in guinea-pig substantia nigra pars compacta neurones. J Physiol. 1993; 466:727–747. [PubMed: 8410714]
23. Ferrari D, Sanchez-Pernaute R, Lee H, Studer L, Isacson O. Transplanted dopamine neurons derived from primate ES cells preferentially innervate DARPP-32 striatal progenitors within the graft. Eur J Neurosci. 2006; 24:1885–1896. [PubMed: 17067292]
24. Olanow CW, Kordower JH, Freeman TB. Fetal nigral transplantation as a therapy for Parkinson's disease. Trends Neurosci. 1996; 19:102–109. [PubMed: 9054056]
25. Zetterström RH, et al. Dopamine neuron agenesis in Nurr1-deficient mice. Science. 1997; 276:248–250. [PubMed: 9092472]

26. Quintana E, et al. Efficient tumour formation by single human melanoma cells. Nature. 2008; 456:593–598. [PubMed: 19052619]

27. Kim H, et al. miR-371-3 Expression Predicts Neural Differentiation Propensity in Human Pluripotent Stem Cells. Cell Stem Cell. 2011; 8:695–706. [PubMed: 21624813]

28. Hargus G, et al. Differentiated Parkinson patient-derived induced pluripotent stem cells grow in the adult rodent brain and reduce motor asymmetry in Parkinsonian rats. Proceedings of the National Academy of Sciences of the United States of America. 2010; 107:15921–15926. [PubMed: 20798034]

29. Aubry L, et al. Striatal progenitors derived from human ES cells mature into DARPP32 neurons in vitro and in quinolinic acid-lesioned rats. Proc Natl Acad Sci U S A. 2008; 105:16707–16712. [PubMed: 18922775]

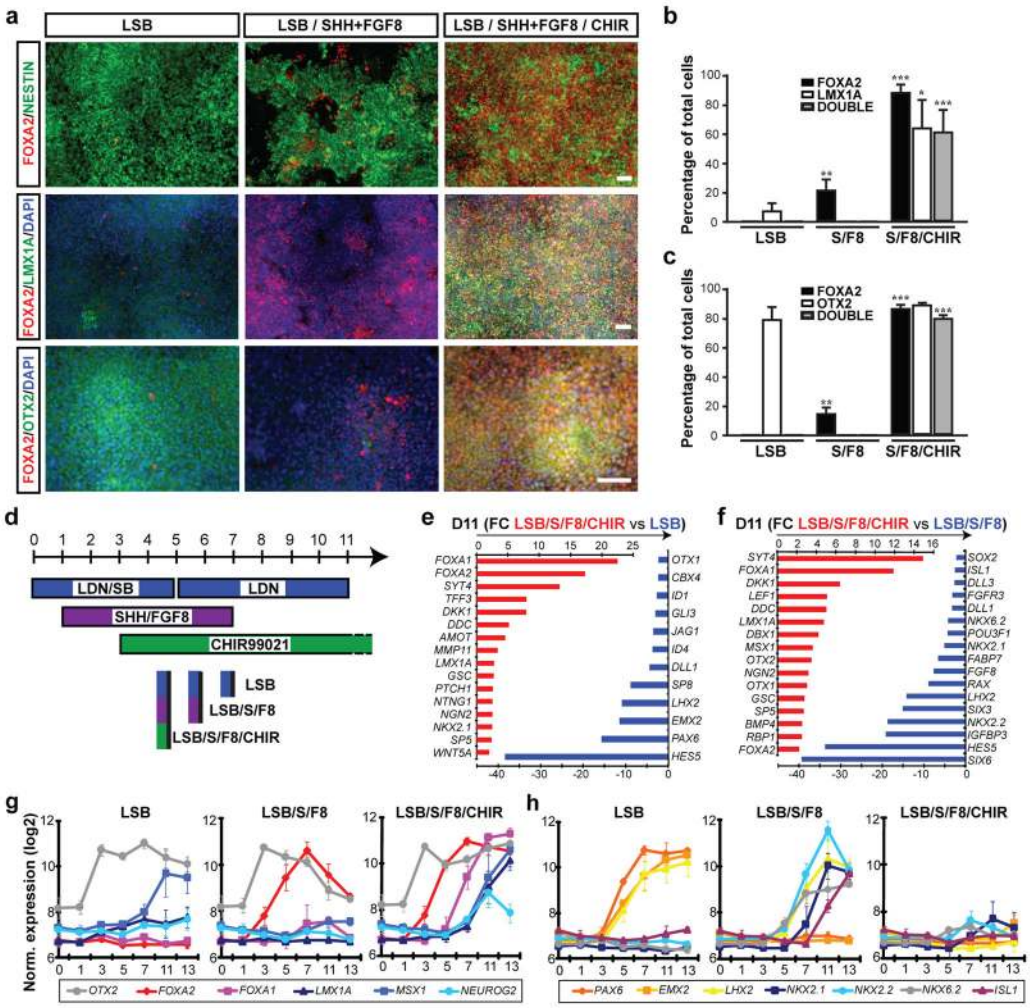


**Figure 1. Induction and neurogenic conversion of hESC-derived midbrain FP precursors is dependent on CHIR99021 addition**

**a**) Immunocytochemistry at day 11 for FOXA2 (red), NESTIN (green, upper panels), LMX1A (green, middle panels) and OTX2 (green, lower panels). **b,c**) Quantification of the data presented in (**a**); mean ± SEM, n=3 (independent experiments): *** $p < 0.001$; ** $p < 0.01$; $p < 0.05$ (compared to LSB, Dunnett test). **d**) Diagram of culture conditions. **e,f**) Selected lists of differentially expressed transcripts at day 11 comparing LSB/S/F8/CHIR versus LSB (**e**) or versus LSB/S/F8 (**f**). **g,h**) Temporal gene expression analysis for markers of midbrain DA precursor (**g**), forebrain and ventral non-DA precursor identity (**h**). Scale bars: 50 μm.

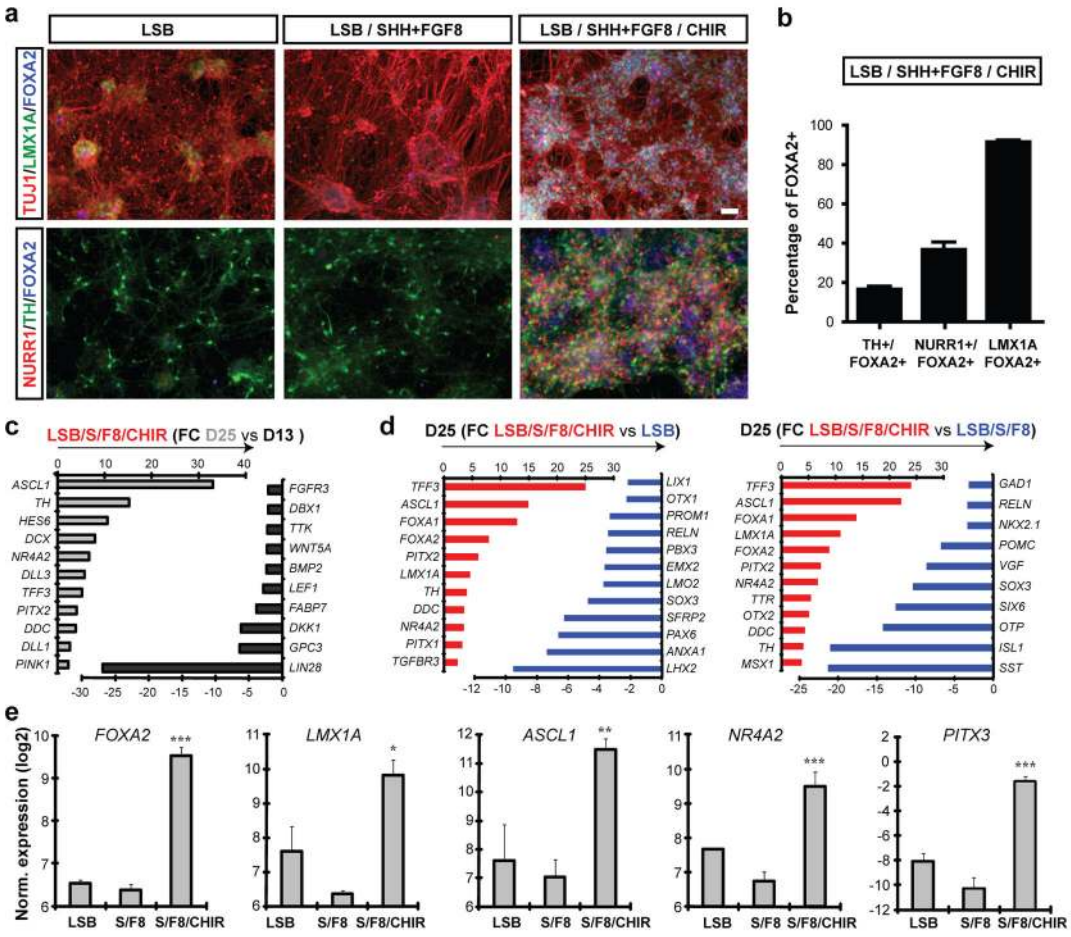


**Figure 2.**

Immunocytochemical and molecular analysis of midbrain DA neuron fate in LSB/S/F8/CHIR treated versus LSB/S/F8 (hypothalamic) and forebrain LSB (dorsal forebrain) fates. **a)** Immunocytochemistry at day 25 for co-expression of FOXA2 (blue) with Tuj1(red)/LMX1A(green) (upper panels) and NURR1(red)/TH(green) (lower panels). **b)** Quantitative co-expression analysis for LSB/S/F8/CHIR; mean ± SEM, n=3 (independent experiments). **c,d)** Global gene expression analysis at day 25 (triplicates each). Selected lists of differentially expressed transcripts comparing day 13 versus day 25 in LSB/S/F8/CHIR **(c)** LSB/S/F8/CHIR versus LSB (**d**, left panel) and LSB/S/F8 (**d**, right panel). **e**) Gene expression analysis for key midbrain DA neuron markers. Significance compared to LSB: Dunnett test: *** $p < 0.001$; ** $p < 0.01$; * $p < 0.05$). Scale bars: 50 μm.

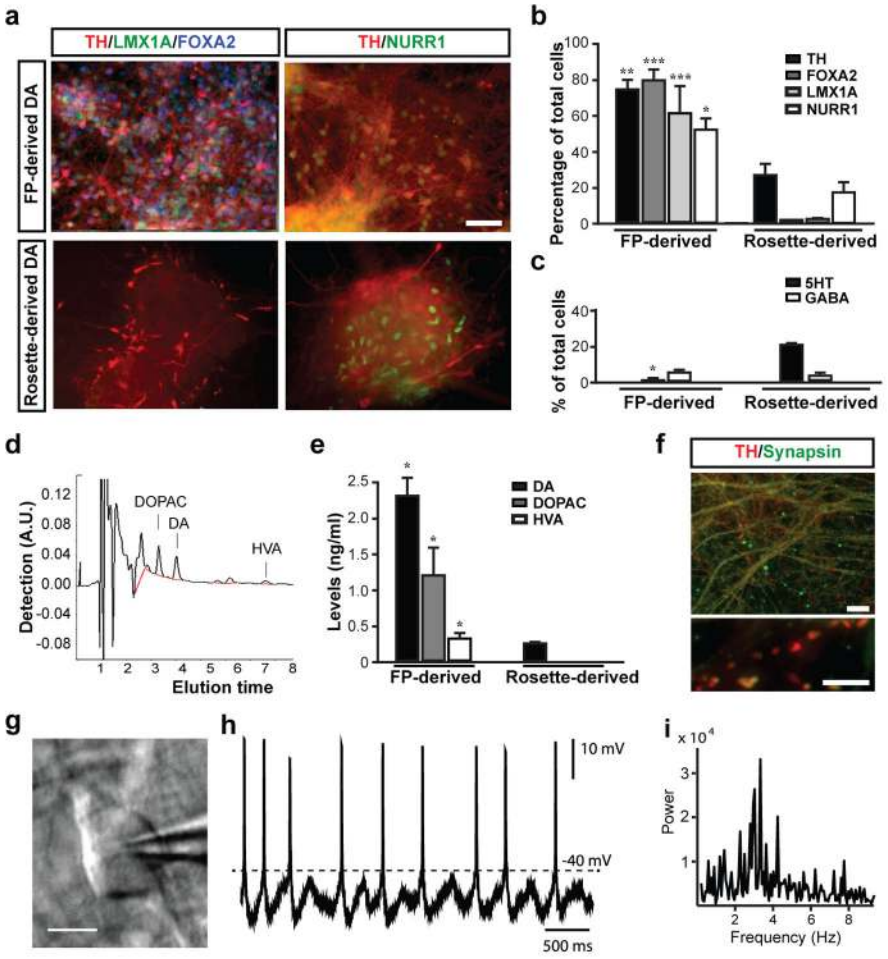


**Figure 3.** ***In vitro*** **maturation and functional characterization of FP versus rosette-derived midbrain DA neurons**

**a**) Immunocytochemistry at day 50 for TH (red), with LMX1A (green) and FOXA2 (blue; left panels) and NURR1 (green, right panels). **b**) Quantification of TH+, FOXA2+, LMX1+ and NURR1+ cells in rosette- versus FP-derived (LSB/S/F8/CHIR) cultures. **c**) Quantification of serotonin+ (5-HT), and GABA+ neuronal subtypes at day 50 in rosette- versus FP-derived cultures. **d,e**) HPLC analysis for DA and metabolites **d**) Representative HPLC chromatogram in a sample of FP-derived cultures. **e**) Levels of DA, DOPAC and HVA in FP-and rosette-derived cultures. **f**) Immunocytochemistry in FP-derived cultures (day 80) for TH (red) and synapsin (green). **g-i**) Electrophysiological analyses of FP cultures at day 80. Phase contrast image of a patched neuron (**g**) and corresponding recordings (**h**). **i**) Power analysis showing membrane potential oscillations characteristic of DA neuron identity (2~5Hz) Mean ± SEM; significance (panels **b, c, e)** comparing FP versus rosette-derived cultures: Student's T-test: *** $p < 0.001$; ** $p < 0.01$; $p < 0.05$). Scale bars: 50 μm in (**a**), 20 μm in (**f**, upper panel), 5 μm in (**f,** lower panel) and 20 μm in (**g**)

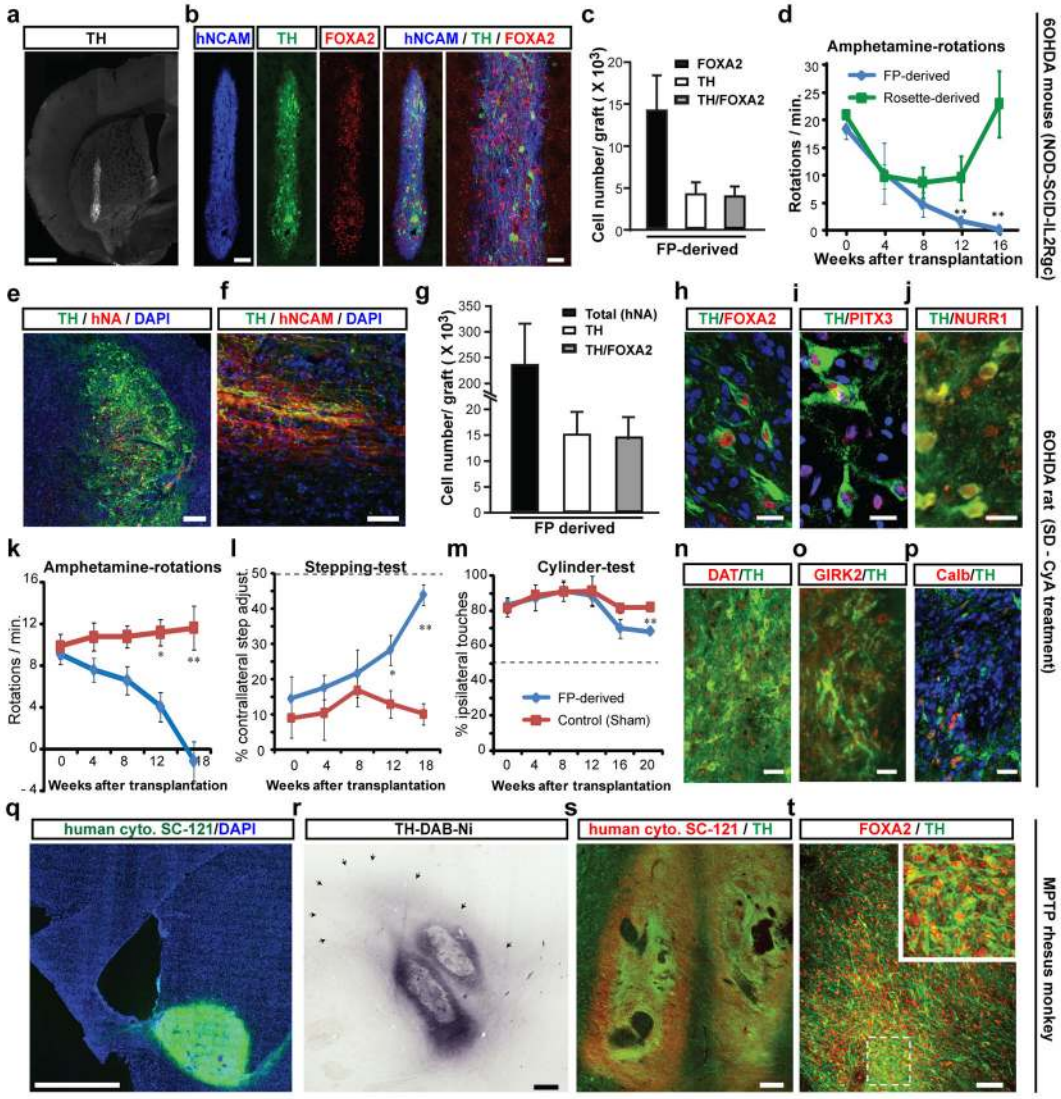


**Figure 4.** ***In vivo*** **survival and function of FP-derived human DA neurons in mouse, rat and monkey PD hosts**

**a-d**) 6-OHDA lesioned adult mice (*NOD-SCID IL2Rgc* null strain): **a**) TH expression and graft morphology at 4.5 months after transplantation. **b**) Expression of human specific marker (hNCAM, blue), TH (green), and FOXA2 (red). **c**) Quantification of FOXA2+ and TH+ cells in FP-derived grafts (mean ± SEM, n=4 at 4.5 months post grafting). **d**) Amphetamine-induced rotation analysis in FP- (blue) versus rosette-derived (green) grafts. Scale bars: 500 μm in (**a**), and 100 and 40 μm in (**b**).

**e-p**) 6-OHDA lesioned adult rats: Immunohistochemistry for TH (green) and human specific markers (red) hNA (**e**) and hNCAM (**f**). **g**) Stereological quantification of hNA+, TH+ and TH+ cells co-expressing FOXA2 (average graft volume = 2.6 ± 0.6 $mm^3$). **h-j**) Co-expression of TH (green) with FOXA2, PITX3 and NURR1 (red). **k-m**) Behavioral analysis in FP- versus sham-grafted animals. **k**) Amphetamine-induced rotational asymmetry. **l**) stepping test: measuring forelimb akinesia in affected versus non-affected side. **m**) Cylinder test: measuring ipsi- versus contra-lateral paw preference. Grafted animals showed

significant improvement in all three tests ($p < 0.01$ at 4.5–5 month; n=4–6 each). **n-p**) Immunohistochemistry for TH (green) and co-expression (red) with DAT (**n**), GIRK2 (**o**) and calbindin (**p**). Significance levels (panels **d, k, l, m)**: ** $p < 0.01$; $p < 0.05$). Scale bars: 200 μm in (**e**), 50 μm in (**f**), 20 μm in (**h-j**) and 40 μm in (**n-p**).

**q-t**) Adult MPTP lesioned rhesus monkeys. **q**) Representative graft at 1 month after transplantation expressing human specific cytoplasm marker SC-121 (green). **r**) TH expression in graft with surrounding TH+ fibers (arrows). **s**) Co-expression of SC-121 (red) and TH (green). **t**) Co-expression of FOXA2 (red) and TH+ (green). Scale bars: 2mm for (**q**), 500 μm for (**r**), 200 μm for (**s**), and 50 μm for (**t**).